

Dynamic friction on rigid and flexible bonds

B. J. Berne, M. E. Tuckerman, John E. Straub, and A. L. R. Bug

Citation: *The Journal of Chemical Physics* **93**, 5084 (1990); doi: 10.1063/1.458647

View online: <http://dx.doi.org/10.1063/1.458647>

View Table of Contents: <http://scitation.aip.org/content/aip/journal/jcp/93/7?ver=pdfcov>

Published by the AIP Publishing

Articles you may be interested in

[Looping and reconfiguration dynamics of a flexible chain with internal friction](#)

AIP Advances **4**, 067102 (2014); 10.1063/1.4881416

[Symplectic dynamics: Limits of particle beams' rigidity and flexibility](#)

AIP Conf. Proc. **1507**, 917 (2012); 10.1063/1.4788988

[Nonlinear dynamic analysis on rigid-flexible coupling system of an elastic beam](#)

Theor. Appl. Mech. Lett. **2**, 023001 (2012); 10.1063/2.1202301

[Density, temperature, and bond-length dependence of dynamic friction on a molecular bond](#)

J. Chem. Phys. **111**, 4698 (1999); 10.1063/1.479231

[A theory for dynamic friction on a molecular bond](#)

J. Chem. Phys. **110**, 6827 (1999); 10.1063/1.478587



Dynamic friction on rigid and flexible bonds

B. J. Berne, M. E. Tuckerman,^{a)} John E. Straub^{b)} and A. L. R. Bug^{c)}
Department of Chemistry, Columbia University, New York, New York 10027

(Received 7 May 1990; accepted 8 June 1990)

A wide variety of problems involving molecular motion in liquids can be formulated in terms of the generalized Langevin equation (GLE). The friction coefficient on a molecular bond or on some more complicated reaction coordinate is then required. An often used approximation is to set the dynamic friction constant equal to the autocorrelation function of the fluctuating force exerted on the frozen bond by the remaining unfrozen coordinates. The true friction involves projection operators and should differ from this approximation. In this paper we derive various identities and show that the rigid bond approximation is the high frequency limit of the true dynamic friction coefficient. We compute the "true" dynamic friction and the friction approximated on the basis of the rigid or frozen bond and show that the asymptotic limit is very accurate even for frequencies not much larger than the peak frequency of the solvent spectral density. Two different dynamical systems are studied using MD simulations with our newly devised NAPA integrator for systems with disparate time scales. In one the molecule is not allowed to rotate and in the other it is allowed to rotate. Interestingly, even for very long rotational reorientation times, small but significant differences in the long time decay of the bond dynamic friction are observed for rotational and nonrotational molecules—differences, however, that do not produce large differences in the static friction constants.

I. INTRODUCTION

A wide variety of problems involving molecular motion in liquids can be formulated in terms of the generalized Langevin equation (GLE).¹⁻³ When this approach is valid (and it is not always valid), it is necessary to know how the dynamic friction coefficient varies with time. It is very difficult to make a purely theoretical calculation of this quantity except in the simple case of the translational⁴ and whole body rotations of rigid molecules.⁵ What is often needed is the friction coefficient on a molecular bond or the friction coefficient on some more complicated reaction coordinate. Various models have been used to describe bond friction. Consider the bond in a homonuclear diatomic molecule. If the bond length is very large compared to the diameters of the solvent atoms (a situation that applies only when the molecule is very close to the dissociation limit) each of the atoms will experience strong forces only from solvent molecules in their vicinity, and because these two sets of proximal solvent atoms are very far apart there will only be small cross correlations in the solvent forces on the two atoms. In this case the friction on the bond will be well approximated by $\zeta_{sp}(t)/2$, where $\zeta_{sp}(t)$ is the dynamic friction on one of the atoms due to its interaction with the fluid. Because the two atoms are far apart this can be corrected using the Oseen form of the hydrodynamic interaction,⁶ but here it is necessary to use the time dependent variant of the Oseen interaction. Neglect of the hydrodynamic interaction gives the well known free-draining limit. This approximation will be valid only if the

bond is very long. When the bond is short each atom of the molecule will experience forces from the same solvent atoms and there will be strong short range cross correlations; moreover, one cannot apply the Oseen form of the hydrodynamic interaction to these problems because this is a far field limit of the true hydrodynamics. Unfortunately it is very difficult to work out theoretical expressions when the intramolecular atoms are near each other. One of the few meaningful attempts to do this, based on a renormalized kinetic theory, shows how difficult this problem is.^{7,8} In light of this, any attempt to deal with a polyatomic in a realistic manner is prohibitively difficult.

Despite these difficulties, there have been many interesting attempts to understand vibrational relaxation, barrier crossing dynamics, and diffusion controlled reactions from this point of view.^{9,10} A popular approach is to simulate the system using stochastic molecular dynamics. In this approach one assumes that each atom in the molecule experiences a random force, and because not much is known about the above mentioned cross correlations, it is assumed that the random forces on each atom are uncorrelated. The random force is modeled as a Gaussian stochastic process with a colored noise spectrum and with a strength given by the single atom memory friction constant. The variant in strong collision models is that each atom on the molecule experiences independent and instantaneous binary collisions.^{11,12} This ignores the fact that two neighboring atoms in the molecule are likely to experience a strong force or a strong collision from the same fluid molecule. Often these models are used without justification, usually for reasons of theoretical expediency. In this paper we test this model against simulation data, and show that it gives a poor approximation to the friction on molecular bonds as might be expected.

Recently, an accurate method for the calculation of time-dependent friction on molecular bonds as a function of

^{a)} Ph.D. student in Department of Physics, Columbia University.

^{b)} Present address: Department of Chemistry, Boston University, Cambridge, Massachusetts 02215.

^{c)} Present address: Department of Physics and Astronomy, Swarthmore College, Swarthmore, Pennsylvania 19081.

the bond length, as well as solvent mass and structure, was presented.^{13,14} This method (is outlined in Sec. IV) has already been used to determine the time-dependent friction for a simple isomerization reaction.¹⁵ Detailed knowledge of the time dependence of the friction was found to be important in making accurate theoretical predictions of the rate constant.

It is usually the case that the oscillator has a high frequency compared to the frequencies characterizing the solvent motion. To apply our methods it is necessary to treat one of the most pervasive problems in the literature on molecular dynamics; that is, the problem of treating systems with high and low frequency motions. Recently we have devised a simple new integrator (NAPA: numerical analytical propagator algorithm) to treat systems with multiple time scales or disparate frequencies numerically.¹⁶ This integrator allows us to determine the dynamic friction, $\zeta(t; \omega_0)$ on a homonuclear diatomic bond as a function of the vibrational frequency ω_0 (for very high frequencies) from simulation. For the first time it becomes possible to evaluate this bond friction and to assess the accuracy of various theoretical approximations for it.

The dynamical system studied in this paper consists of a harmonic oscillator dissolved in a Lennard-Jones (6-12) fluid with which the diatomic interacts through a site-site LJ potential with the solvent atoms with the same parameters as used for the solvent-solvent potential.

Section II of this paper provides a detailed analytic treatment of the dynamic friction on the bond. The analysis is based on the case where the molecule is not allowed to rotate. It is difficult to include the rotations because of difficulties in performing the analysis in angle space. Nevertheless, we show in Sec. IV that in dense fluids, where the rotations are hindered on the time scale of the force correlation time, this analysis is applicable to the full problem. We derive an expression for the bond friction, Eq. (2.7), and in Sec. IV we use our simulation methods to determine this quantity. We also show that when the bond frequency, ω_0 , is very high compared to the frequencies of motion of the solvent, the asymptotic result given by Eq. (3.17) should be an excellent approximation to the true friction. This latter result requires only the determination of the autocorrelation function of the force exerted by the solvent on the bond when the bond is held rigidly fixed at the bond length for the molecule in vacuum. Although this rigid bond friction approximation has been used before by others¹⁷ no derivation of it has been given and no assessment of its accuracy was available. A derivation and assessment is provided in this paper. The question to be answered here is: How good is this rigid molecule approximation? In this paper we show that, even for relatively low vibrational frequencies, the asymptotic result, Eq. (3.17), appears to be an excellent approximation—a result that was unanticipated. A further test of this idea is to use the GLE to calculate the absorption spectrum of the diatomic molecule using the spectral resolution of the rigid-bond dynamic friction. It is found that this gives excellent agreement with MD. When the free-draining friction is used the resulting spectrum is in poor agreement with MD. By-products of the formal analysis of the GLE are a suggestion

of yet another way to determine the exact dynamic friction from unprojected dynamics and a demonstration of how MD can be used to test whether the bath is Ohmic or non-Ohmic.

The GLE for a molecule not allowed to rotate is much simpler than for a molecule allowed to rotate. In very dense fluids molecular rotations are hindered and the reorientational relaxation times are very long. One might imagine that the friction on the molecular bonds will be different for rotational and nonrotational molecules. If the molecule rotates or librates the solvent force on intramolecular bonds will fluctuate due to the rotations. In this paper we compare the molecular dynamics for the rotational and nonrotational molecules in very dense fluids and find that there are subtle but small differences that will effect the static friction coefficient. Of course for more dilute fluids where the tumbling times get small these differences should grow.

II. ANALYTICAL THEORY OF DYNAMIC FRICTION ON A HARMONIC BOND

It is straightforward application of projection operator techniques to treat the dynamics of a harmonic oscillator in a bath.^{1,18–21} If

$$\mathbf{A} = \begin{pmatrix} q \\ p \end{pmatrix}, \quad (2.1)$$

denotes the state of the oscillator where $q = x - \bar{x}$, p is the conjugate momentum, and $P = (\dots, \mathbf{A}^+) (\mathbf{A}, \mathbf{A}^+)^{-1} \mathbf{A}$ denotes a projection operator onto \mathbf{A} , one can derive the following generalized Langevin equation for \mathbf{A} ,

$$\dot{\mathbf{A}} = i\Omega \mathbf{A}(t) - \int_0^t d\tau \mathbf{K}(\tau) \mathbf{A}(t - \tau) + \mathbf{F}(t), \quad (2.2)$$

where $(\mathbf{A}, \mathbf{A}^+)$ is the canonical equilibrium average, $\langle \mathbf{A} \mathbf{A}^+ \rangle$, the frequency matrix is defined as

$$i\Omega = \begin{pmatrix} 0 & 1/\mu \\ -\mu\tilde{\omega}^2 & 0 \end{pmatrix}. \quad (2.3)$$

$\mathbf{F}(t)$ is the random force, $Q = 1 - P$ is a projector onto the orthogonal complement of \mathbf{A} , and $L = -i\{\dots, H\}$ is the Liouville operator.

$$\mathbf{F}(t) = e^{iQLt} Q iL \mathbf{A} = e^{iQLt} \begin{pmatrix} 0 \\ \dot{p} + \mu\tilde{\omega}^2 q \end{pmatrix}, \quad (2.4)$$

and the memory function matrix is

$$\mathbf{K}(t) = (\mathbf{F}(t), \mathbf{F}(0)^+) (\mathbf{A}(0), \mathbf{A}^+(0))^{-1} \quad (2.5)$$

or

$$\mathbf{K}(t) = \begin{pmatrix} 0 & 0 \\ 0 & \zeta(t)/\mu \end{pmatrix}. \quad (2.6)$$

$\zeta(t)$ in Eq. (2.6) is the dynamic friction coefficient which has the explicit form

$$\frac{\zeta(t)}{\mu} = \frac{\langle \delta f e^{iQLt} \delta f \rangle}{\langle p^2 \rangle}, \quad (2.7)$$

with

$$\delta f \equiv \dot{p} + \mu\tilde{\omega}^2 q = -\frac{\partial V}{\partial x} + \mu\tilde{\omega}^2 (x - \langle x \rangle), \quad (2.8)$$

and $\tilde{\omega}^2$ is given by

$$\tilde{\omega}^2 = [\beta\mu\langle q^2 \rangle]^{-1}, \quad (2.9)$$

where both $\langle x \rangle$ and $\langle q^2 \rangle$ depend on x_0 , ω_0 , and the forces exerted by the bath on the reaction coordinate x including centrifugal distortion.

Equation (2.2) can also be written in component form as,

$$\begin{aligned} \frac{dq}{dt} &= \frac{p}{\mu} \\ \frac{dp}{dt} &= -\mu\tilde{\omega}^2 q(t) - \int_0^t d\tau \zeta(\tau) \dot{q}(t-\tau) + F(t), \end{aligned} \quad (2.10)$$

where

$$F(t) = e^{iQLt} \delta f \quad (2.11)$$

is the random force acting on the displacement q . These equations rigorously describe the dynamics of small fluctuations from equilibrium.

Equation (2.7) shows that $\zeta(t)$ involves the propagator e^{iQLt} which contains the projection operator Q . It is possible to express $\zeta(t)$ in terms of the time correlation function

$$\frac{\phi(t)}{\mu} = \frac{\langle \delta f e^{iLt} \delta f \rangle}{\langle p^2 \rangle}, \quad (2.12)$$

which involves the propagator e^{iLt} and is thus determined by pure Hamiltonian flow. To derive this relationship we define the correlation matrix

$$\frac{\Phi(t)}{\mu} = (e^{iLt} \mathbf{F}(0), \mathbf{F}(0)^+) (\mathbf{A}, \mathbf{A}^+)^{-1}, \quad (2.13)$$

or

$$\frac{\Phi(t)}{\mu} = \begin{pmatrix} 0 & 0 \\ 0 & \phi(t)/\mu \end{pmatrix}. \quad (2.14)$$

From Eqs. (2.5) and (2.14) we see that $\Phi(t)$ and $\mathbf{K}(t)$ differ only with respect to the propagator: where the former has e^{iLt} , the latter has e^{iQLt} .

It is a straightforward but tedious matter to derive the relationships between $\tilde{\mathbf{K}}(s)$ and $\tilde{\Phi}(s)$ which are the Laplace transforms of $\mathbf{K}(t)$ and $\Phi(t)$ respectively. The basic approach is given in Berne and Pecora¹ Eq. (11 B 2), although there is a typo reversing the order of the matrices. The result is

$$\tilde{\mathbf{K}}(s) = \tilde{\Phi}(s) [\mathbf{I} - (s\mathbf{I} - i\Omega)^{-1} \tilde{\Phi}(s)]^{-1}. \quad (2.15)$$

This can also be expressed as,

$$\tilde{\Phi}(s) = \tilde{\mathbf{K}}(s) - \tilde{\mathbf{K}}(s) [s\mathbf{I} - i\Omega + \tilde{\mathbf{K}}(s)]^{-1} \tilde{\mathbf{K}}(s). \quad (2.16)$$

Substituting in the matrices $\tilde{\Phi}(s)$ and $\tilde{\mathbf{K}}(s)$ and $i\Omega$ from Eqs. (2.14), (2.6) and (2.3) allows us to write

$$\frac{\tilde{\zeta}(s)}{\mu} = \frac{[\tilde{\phi}(s)/\mu]}{1 - \{[s/(s^2 + \tilde{\omega}^2)] [(\tilde{\phi}(s)/\mu)]\}}, \quad (2.17)$$

or

$$\frac{\tilde{\phi}(s)}{\mu} = \frac{[\tilde{\zeta}(s)/\mu]}{1 + \{[s/(s^2 + \tilde{\omega}^2)] [(\tilde{\zeta}(s)/\mu)]\}}. \quad (2.18)$$

Taking the $\lim_{s \rightarrow 0} \tilde{\zeta}(s)$ gives for $\tilde{\omega} > 0$

$$\lim_{s \rightarrow 0} \tilde{\zeta}(s) = \lim_{s \rightarrow 0} \tilde{\phi}(s). \quad (2.19)$$

The left-hand side of this expression is the static friction constant ζ_0

$$\zeta_0 = \frac{1}{kT} \int_0^\infty dt \langle \delta f e^{iQLt} \delta f \rangle. \quad (2.20)$$

From the right-hand side of the equality in Eq. (2.19) it follows that when $\tilde{\omega} > 0$

$$\zeta_0 = \frac{1}{kT} \int_0^\infty dt \langle \delta f e^{iLt} \delta f \rangle, \quad (2.21)$$

a quantity that involves pure Hamiltonian flow and that can be readily calculated from the MD trajectories. This gives a direct method for determining the static friction. Alternatively straight MD trajectories can be used to determine $\phi(t)$. Laplace transformation of this result followed by substitution into Eq. (2.17) followed by inverse Laplace transformation gives the desired dynamic friction coefficient. In subsequent sections we use our former MD method¹³ to determine $\zeta(t)$. Nevertheless, it is worth noting that this approach can also be used.

When the bath gives rise to Ohmic dissipation, $\zeta_0 > 0$, it follows that $\tilde{\phi}(0) > 0$ whereas when the bath gives non-Ohmic dissipation, $\zeta_0 = 0$ and $\tilde{\phi}(0) = 0$. Thus when $\tilde{\omega} > 0$, molecular dynamics can be used to determine whether the bath is Ohmic or non-Ohmic, according to:

$$\int_0^\infty dt \langle \delta f e^{iLt} \delta f \rangle = \begin{cases} > 0 & \text{Ohmic} \\ = 0 & \text{non-Ohmic.} \end{cases} \quad (2.22)$$

It is interesting to note that for free motion (as opposed to harmonic motion $\tilde{\omega} = 0$, and Eq. (2.17) reduces to

$$\frac{\tilde{\zeta}(s)}{\mu} = \frac{[\tilde{\phi}(s)/\mu]}{1 - \{[1/s] (\tilde{\phi}(s)/\mu)\}} \quad (2.23)$$

in which case if $\zeta_0 > 0$, $\tilde{\phi}(0) = 0$ and if $\tilde{\zeta}(0) = 0$ it follows that $\tilde{\phi}(0) \neq 0$. Then the conditions are reversed from the harmonic system given in Eq. (2.22).

Another thing we learn from Eq. (2.17) is that when ω_0 (and $\tilde{\omega}$) are much larger than all the frequencies in the bath and $\tilde{\omega} \gg \zeta_0$, it follows that

$$\begin{aligned} \lim_{\omega_0 \rightarrow \infty} \frac{\tilde{\zeta}(s)}{\mu} \\ = \lim_{\omega_0 \rightarrow \infty} \frac{[\tilde{\phi}(s)/\mu]}{1 - \{[s/(s^2 + \tilde{\omega}^2)] [(\tilde{\phi}(s)/\mu)]\}} = \lim_{\omega_0 \rightarrow \infty} \frac{\tilde{\phi}(s)}{\mu}. \end{aligned} \quad (2.24)$$

Thus for a very high frequency harmonic motion the projection operator Q disappears from the correlation function. Denoting this limit by $\tilde{\zeta}^{(\infty)}(s)$ and $\tilde{\phi}^{(\infty)}(s)$ we get

$$\tilde{\zeta}^{(\infty)}(t) = \lim_{\omega_0 \rightarrow \infty} \frac{1}{kT} \langle \delta f e^{iLt} \delta f \rangle, \quad (2.25)$$

and the dynamic friction can be derived from the Hamiltonian flow (i.e., with no Q in the propagator).

A simple model illustrates this. Let $\zeta(t) = \zeta(0)e^{-\gamma t}$; or equivalently $\tilde{\zeta}(s) = \zeta(0)/(s + \gamma)$. Substituting this into Eq. (2.18) and solving for the case $\tilde{\omega} \gg \zeta(0)$ and $\tilde{\omega} \gg \gamma$ by perturbation solution of the dispersion equation

$$s^2 + \tilde{\omega}^2 + s \frac{\tilde{\zeta}(s)}{\mu} = 0$$

shows that to leading order, $\phi(t) = \zeta(0)e^{-\gamma t} = \zeta(t)$ as expected from Eq. (2.24).

III. HIGH FREQUENCY LIMIT

In this section we will show that if the system consists of a diatomic molecule then $\zeta^{(\infty)}(t)$ will be given by the autocorrelation function of the force on the bond of a rigid molecule. This gives a high frequency asymptotic approximation to the true friction $\zeta(t)$ on a nonrigid bond.

$$\zeta^{(\infty)}(t) = \frac{1}{kT} \langle [f^{(0)} - \bar{f}^{(0)}] e^{iL_s t} [f^{(0)} - \bar{f}^{(0)}] \rangle, \quad (3.1)$$

where $f^{(0)}$ is the force on the oscillator coordinate when it is fixed at a bondlength x_0 , $\bar{f}^{(0)}$ is its average value, and $e^{iL_s t}$ is the unprojected propagator of the whole system with the bond thus constrained. If the system consists of a diatomic molecule, then Eq. (3.1) is the autocorrelation function of the force on the bond of a rigid molecule. This will give an approximation to the true friction $\zeta(t)$ on a non rigid bond. Later in this paper we shall assess the accuracy of this approximation.

To derive this result we find it convenient to use action angle variables for the harmonic oscillator and to use the adiabatic theorem of classical mechanics. Pechukas²² has lucidly outlined how to treat a dynamical system in which there is a high frequency classical oscillator coupled to a slowly moving bath. Following Pechukas, let \mathbf{R} be the slow degrees of freedom of the liquid, with conjugate momenta \mathbf{P} , interacting with the high frequency, one dimensional oscillator with coordinate x (bond length), equilibrium bond length x_0 and momentum p according to the Hamiltonian:

$$H = H_0(\mathbf{P}, \mathbf{R}) + h(p, x, \mathbf{R}). \quad (3.2)$$

Here H_0 is the pure solvent Hamiltonian and h is the Hamiltonian of the oscillator containing its coupling to the liquid. Let

$$I(\epsilon, \mathbf{P}) = \frac{1}{2\pi} \oint p dq \quad (3.3)$$

be the action, for fixed \mathbf{R} , as a function of the oscillator energy ϵ ; the integral is over one complete cycle of oscillation. The coordinate conjugate to I will be an angle α . Equation (3.3) can be inverted to give the oscillator energy as a function of I for fixed \mathbf{R} . The classical Born–Oppenheimer approximation then consists in replacing the Hamiltonian given in Eq. (3.2) by the Hamiltonian:

$$\bar{H} = H_0(\mathbf{P}, \mathbf{R}) + \epsilon(I, \mathbf{R}) \quad (3.4)$$

and regarding I as the oscillator momentum, conjugate to a cyclic coordinate. We are interested in the case when the oscillator period is very short ($\omega_0 \rightarrow \infty$) compared to the times over which \mathbf{P} and \mathbf{R} change significantly. In this case the dynamics generated by \bar{H} very accurately generates the full dynamics generated by H . In this limit $\dot{I} = -\partial \bar{H} / \partial \alpha = 0$ and $\dot{\alpha} = \partial \bar{H} / \partial I = \omega(I, \mathbf{R})$. In this limit

the Liouvillian, $iL = \{\cdots, H\}$ for the full dynamical system defined by Eq. (3.2) is replaced by the Liouvillian $iL_I = \{\cdots, \bar{H}\}$ corresponding to the Hamiltonian averaged over one cycle of the oscillator defined by Eq. (3.4), and the propagator becomes:

$$\exp iL t \rightarrow \exp i\bar{L}_I t. \quad (3.5)$$

The oscillator Hamiltonian

$$h(p, x, \mathbf{R}) = \frac{p^2}{2m} + \frac{1}{2} \mu \omega_0^2 (x - x_0)^2 + v(x, \mathbf{R}) \quad (3.6)$$

in Eq. (3.2) can be expanded in a power series in $(x - x_0)$. For sufficiently high unperturbed frequency ω_0 the displacement $(x - x_0)$ will be very small and it is expected that this power series can be truncated after the quadratic term without seriously affecting the dynamics. After completing the squares, $h(p, x, \mathbf{R})$ takes the form

$$h(x, p, \mathbf{R}) = \frac{p^2}{2m} + \frac{1}{2} \mu \Omega(\mathbf{R})^2 (x - x_0 - a(\mathbf{R}))^2 + V(x_0, \mathbf{R}), \quad (3.7)$$

where

$$\mu \Omega^2(\mathbf{R}) = \mu \omega_0^2 + \left(\frac{\partial^2 v(x, \mathbf{R})}{\partial x^2} \right)_{x=x_0}, \quad (3.8)$$

$$a(\mathbf{R}) = \frac{f^{(0)}(x_0, \mathbf{R})}{\mu \Omega^2(\mathbf{R})}, \quad (3.9)$$

$$f^{(0)}(\mathbf{R}) = - \left(\frac{\partial v(x, \mathbf{R})}{\partial x} \right)_{x=x_0}, \quad (3.10)$$

and

$$V(x_0, \mathbf{R}) = v(x_0, \mathbf{R}) - \frac{1}{2} \frac{[f^{(0)}(\mathbf{R})]^2}{\mu \Omega^2(\mathbf{R})}. \quad (3.11)$$

Transforming to action-angle variables:

$$x = x_0 + a(\mathbf{R}) + [2L / \mu \Omega(\mathbf{R})]^{1/2} \sin \alpha \quad (3.12)$$

$$p = [2mI\Omega(\mathbf{R})]^{1/2} \cos \alpha$$

allows one to write the Hamiltonian \bar{H} as

$$\bar{H} = H_0(\mathbf{P}, \mathbf{R}) + V(x_0, \mathbf{R}) + \Omega(\mathbf{R})I. \quad (3.13)$$

Likewise the fluctuating force defined by Eq. (2.8) can be expressed as

$$\delta f = \delta f(x_0 + a(\mathbf{R}) + [2I / \mu \Omega(\mathbf{R})]^{1/2} \sin \alpha, \mathbf{R}). \quad (3.14)$$

Substitution of these action angle variables and the Born–Oppenheimer equation Eq. (3.5) into the time correlation function $\zeta^{(\infty)}(t)$ of Eq. (2.25) gives

$$\zeta^{(\infty)}(t) = \lim_{\omega_0 \rightarrow \infty} \frac{1}{kT} \langle \delta f e^{i\bar{L}_I t} \delta f \rangle, \quad (3.15)$$

or

$$\zeta^{(\infty)}(t) = \lim_{\omega_0 \rightarrow \infty} \frac{1}{kT} \frac{\int d\mathbf{R} \int d\mathbf{P} \int dI e^{-\beta \bar{H}} \delta f e^{i\bar{L}_I t} \delta f}{\int d\mathbf{R} \int d\mathbf{P} \int dI e^{-\beta \bar{H}}}. \quad (3.16)$$

We proceed by noting that the average indicated by the angular brackets in Eq. (3.15) indicates an average over a canonical distribution function with the Hamiltonian of Eq.

(3.13). In the limit $\omega_0 \rightarrow \infty$, $\Omega \rightarrow \infty$, and from Tauberian theorems applied to the Laplace transforms, it is clear that wherever the action I appears in the integrals of Eq. (3.16) it must be set equal to zero. This eliminates the angle α from all the terms, and since $a(\mathbf{R}) \rightarrow 0$ for $\omega_0 \rightarrow \infty$ allows one to replace δf by $[f^{(0)} - \bar{f}^{(0)}]$, where $f^{(0)}$ is the force exerted by fluid on the bond held rigid at bond length x_0 . When this last result is substituted in Eq. (3.16), we find

$$\xi^{(\infty)}(t) = \frac{1}{kT} \langle [f^{(0)} - \bar{f}^{(0)}] e^{iL_s t} [f^{(0)} - \bar{f}^{(0)}] \rangle, \quad (3.17)$$

where we have implicitly taken into account that $\bar{L}_{I=0}$ is the Liouvillian corresponding to the bond being frozen at bond length x_0 ; that is, $L_s = \bar{L}_{I=0}$. Thus the dynamic friction on a very high frequency bond should be very well approximated by the dynamic friction on a frozen bond of bond length x_0 .

It is interesting to compare this result with what is expected if the Hamiltonian is purely quadratic

$$V = \frac{1}{2} \mu \tilde{\omega}^2 (x - x_0)^2 + \sum_{\alpha=1}^N \frac{1}{2} m_{\alpha} \omega_{\alpha}^2 \left(x_{\alpha} - \frac{g_{\alpha}^2}{m_{\alpha} \omega_{\alpha}^2} x \right)^2. \quad (3.18)$$

As shown by Zwanzig,²³ it is a simple matter to algebraically eliminate the bath modes x_{α} from the equations of motion based on this Hamiltonian and to derive the GLE. The dynamical friction coefficient is given explicitly by,

$$\xi(t) = \sum_{\alpha=1}^N \frac{g_{\alpha}^2}{m_{\alpha} \omega_{\alpha}^2} \cos(\omega_{\alpha} t) = \int_0^{\infty} d\omega J(\omega) \cos(\omega t), \quad (3.19)$$

where g_{α} is the coupling strength and $J(\omega)$ is the spectral density in the continuum limit. It is also a simple matter to show that, if in Eq. (3.18) the bond x is fixed, the autocorrelation function of the property $\delta f \equiv F_x + \mu \tilde{\omega}^2 (x - \bar{x})$ subject to fixed bond length is

$$\begin{aligned} \beta \langle \delta f(0) \exp(iL_{\text{xfixed}} t) \delta f(t) \rangle \\ = \sum_{\alpha=1}^N \frac{g_{\alpha}^2}{m_{\alpha} \omega_{\alpha}^2} \cos(\omega_{\alpha} t) = \xi(t), \end{aligned} \quad (3.20)$$

where L_{xfixed} is the Liouvillian for the system with x fixed. Thus in this harmonic bath approximation the dynamical friction $\xi(t)$ is exactly equal to the autocorrelation function of δf for the system with the bond constrained at any length. This means that for the harmonic bath it is a rigorous result that one can calculate the friction by choosing a rigid reference system—a result that was only asymptotically correct in using the real Hamiltonian [see Eq. (3.17)]. Deutch and Silbey recognized that this constrained reference system could be used to calculate the friction in harmonic systems.²⁴ Later in the paper we use MD simulations to study the dependence of the friction on the impurity oscillator frequency.

IV. MOLECULAR DYNAMICS METHODS AND RESULTS

A. Determination of the dynamic friction coefficient

In previous papers,^{13,14} we applied a very simple method for determining $\xi(t)$ for any given reaction coordinate and applied this method to the calculation of the friction on a diatomic molecular bond embedded in a classical Lennard-Jones liquid. This method is based on the following steps:

(a) The potential function for the coordinate of interest is replaced by a harmonic potential

$$U^{(0)}(x; x_0, \omega_0) = \frac{1}{2} \mu \omega_0^2 (x - x_0)^2 \quad (4.1)$$

with frequency ω_0 , and equilibrium displacement x_0 .

(b) The generalized Langevin equation Eq. (2.10) is multiplied by $\dot{q}(0)$, averaged over a canonical ensemble. Remembering that $\langle R(t) \dot{q}(0) \rangle = 0$, this procedure yields an equation for the velocity autocorrelation function $C_v(t)$

$$\dot{C}_v(t) = - \int_0^t d\tau K(\tau) C_v(t - \tau), \quad (4.2)$$

where the memory function is

$$K(t) = \tilde{\omega}^2 + \frac{\xi(t)}{\mu}. \quad (4.3)$$

These quantities depend parametrically on x_0 and ω_0 . $C_v(t)$ is now determined from molecular dynamics simulations replacing the true intramolecular potential for x by the harmonic potential, $U^{(0)}(x; x_0, \omega_0)$. Equation (4.3) is then numerically solved for $K(t)$ using the method of Berne and Harp²⁵ (or an equivalent method). If, furthermore, $\langle x \rangle$ and $\langle q^2 \rangle$ are determined in the same simulation, $\tilde{\omega}^2$ [defined by Eq. (2.9)] can be calculated.

(c) Substitution of $K(t)$ and $\tilde{\omega}$ into Eq. (4.3) yields $\xi(t)$.

This can be repeated for different values of ω_0 for a given x_0 , and for different values of x_0 . Writing

$$\xi(t) = \xi(t; x_0, \omega_0) \quad (4.4)$$

indicates the parametric dependence of the friction on x_0 and ω_0 .

B. Numerical integration of the equations of motion

The evaluation of the friction on very high frequency oscillators can be performed using standard integrators like the velocity Verlet integrator.²⁶ Standard integrators are stable only if the time step used is short compared to the shortest period in the system. At high vibrational frequencies there is a separation of time scales between the solute and the host fluid. Standard integrators then require the use of a very short time step and consequently a very large number of iterations to sample the requisite number of fluctuations in the force exerted on the solute molecule by the relatively slowly moving solvent. Fortunately, we have recently been able to devise a new integrator¹⁶ called NAPA based on the vibrational motion of the free molecule to integrate the canonical equations of motion for the molecule plus solvent using a much larger time step. For example, for a diatomic with harmonic frequency of 300 (in LJ units) dissolved in a LJ solvent whose peak frequency in the spectral density function is around $\omega_{\text{peak}} = 20$ (in LJ units), we

are able to use a time step 8×10^{-4} instead of a time step of 1×10^{-4} required for straightforward use of the Verlet integrator. Clearly NAPA allows use of time steps an order of magnitude larger than standard integrators.

The system simulated consists of a single homonuclear diatomic molecule A_2 dissolved in a solvent consisting of 62 atoms A . The solute-solvent interaction potential is taken to be a site-site LJ (12-6) potential and the solvent-solvent potential is taken to be pairwise additive with atom-atom interactions also given by the same LJ (12.6) potential; that is a LJ potential with the same ϵ and σ . The intramolecular potential is taken to be either harmonic as specified in Eq. (4.1) or rigid. The system is solved subject to cubic periodic boundary conditions using the NAPA integrator for the harmonic potential or the RATTLE²⁷ version of the SHAKE^{28,29} algorithm for the rigid molecule. For the case of the flexible molecule the method outlined in the beginning of this section is used to determine the dynamical friction; whereas, for the rigid molecule Eq. (3.17) is used to determine the dynamic friction. Solvent forces parallel and perpendicular to the instantaneous bond direction $\hat{r}_{12}(t)$, are calculated at each step. $F_i(t)$ is the force on atom i at time t , then the force on the rigid bond is

$$f^{(0)}(t) = \frac{1}{2} (F_1(t) - F_2(t)) \cdot \hat{r}_{12}(t), \quad (4.5)$$

where $f^{(0)}$ is the force on the rigid bond appearing in Eq. (3.17). The factor of $1/2$ in Eq. (4.5) arises because the mass associated with the coordinate is the reduced mass of the diatomic. $\delta f^{(0)}(t) = f^{(0)}(t) - f^{(0)}(0)$ is then autocorrelated by time averaging over a molecular dynamics trajectory.

All of the simulations are done at a reduced temperature of $\hat{T} = k_B T / \epsilon = 2.5$ and a reduced density of $\hat{n} = \rho \sigma^3 = 1.05$. Simulations were done for molecules of bare harmonic frequencies of $\omega_0 = 20, 30, 60$, and 90 in LJ units $(\epsilon/m\sigma^2)^{1/2}$. In all of these cases $x_0 = 1.25$. Since the analysis of the last section rigorously applies to the case where the molecule does not rotate we simulate systems constrained such that the diatomic is not allowed to rotate. We call these simulations nonrotational dynamics. We also perform simulations for the case where the molecule is allowed to rotate. For both the rotational and the nonrotational flexible molecule NAPA is used; however for the lower frequency flexible rotational molecule ($\omega_0 = 20$ and 30) straight velocity Verlet is used.³⁰ In the Appendix we show how NAPA is applied when there are rotations. The simulations required on the order of 2.5×10^6 time steps.

As indicated in the previous subsection, the friction on the harmonic bond is computed from the velocity autocorrelation function by numerical inversion of the Volterra equation Eq. (4.2). Since the diatomic is a single impurity in the neat Lennard-Jones liquid, a very long run is necessary to obtain a good correlation function. For the cases of $\omega = 20$ and 30 , the run lengths were 2×10^6 steps using a time step of 2×10^{-3} . For $\omega = 60$, it was found that if straightforward velocity Verlet integration was used, energy conservation tolerance required a time step of 1×10^{-3} . For $\omega = 90$, the time step was found to be 6.67×10^{-4} . The run lengths for these two time steps would be 4×10^6 and 6×10^6 steps, respectively. However, using NAPA, it was found that the

same energy conservation could be obtained using time steps of 1.75×10^{-3} for $\omega = 60$, and 1.5×10^{-3} for $\omega = 90$. The run lengths required by these time steps were 2.29×10^6 and 2.67×10^6 steps, respectively. We see that the larger the frequency of the bond, the more efficient the NAPA integration method becomes. The numerical inversion of the Volterra equation is an unstable process and requires closely spaced points in $C_v(t)$. When NAPA is used, we find that the points are not spaced closely enough because of the large time step. However, a forward Euler scheme can be used to obtain velocity points in between NAPA steps. This scheme is based on the simple Taylor series approximation

$$v(h) = v(0) + ha(0), \quad (4.6)$$

where $a(0)$ is the acceleration at the beginning of the step. This method, together with the corresponding backward Euler scheme, was used with NAPA to calculate two velocity points in between each NAPA step. For the case of the rigid bond, a run length of 2×10^6 steps was carried out using a time step of 2×10^{-3} , and the autocorrelation function of the force along the bond was computed. Because of the large number of velocity points required in the $\omega = 90$ case, the FFT method proposed by Futrelle and McGinty was used to compute the velocity autocorrelation function.³¹ Using this method, one computes the Fourier transform of the velocity along the bond as the simulation is running. This requires less disk space, as it is not necessary to store the entire trajectory. The velocity autocorrelation function is computed by an inverse FFT of the square of the velocity transform.

C. Numerical results

First, we discuss the case where the molecule is not allowed to rotate. The velocity autocorrelation function for the vibrational coordinate, $C_v(t)$, for the four frequencies ($20, 30, 60$, and 90) are shown in Fig. 1. To see how the range of frequencies we studied compares to the range of frequencies of the solvent, we plot the spectral density of the velocity of a solvent atom in Fig. 2(a). This plot is based on an analytic fit to the single particle friction kernel [see Eq. (2.6) in Straub *et al.*¹⁵]. This plot shows that the solvent spectral density peaks at 20 and that frequencies greater than 90 contribute negligibly to the spectral density. Thus, for oscillator frequencies in this range, significant dephasing occurs only after very long times. The effects of the frequency disparity can also be seen by plotting the absorption spectrum of the bond in the liquid. This is obtained from the Fourier cosine transform of the velocity autocorrelation function

$$I(\omega) = \int_0^\infty C_v(t) \cos \omega t dt. \quad (4.7)$$

$I(\omega)$ for the four frequencies studied in Fig. 1 are plotted in Fig. 2(b). Note how the full width at half maximum, $\Delta\omega_{FWHM}$, decreases with vibrational frequency, ω_0 . This is plotted in Fig. 3.

The method outlined in the beginning of this section was used to determine the dynamic friction coefficient, $\zeta(t)$ on a flexible (i.e., vibrating), nonrotating bond with $x_0 = 1.25$. For comparison a simulation of a rigid nonrotating diatomic molecule with bond length $x_0 = 1.25$ was carried out. In Fig.

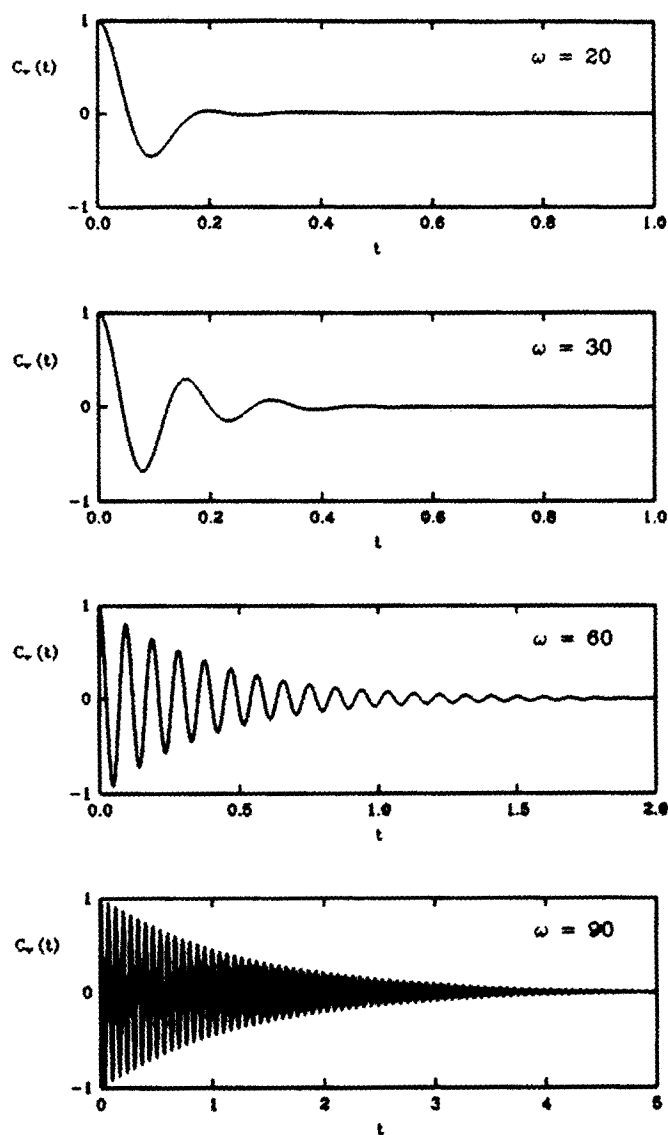


FIG. 1. Velocity autocorrelation functions normalized by the initial value for the nonrotational harmonic diatomic molecule in Lennard-Jonesium ($\hbar = 1.05$ $\bar{T} = 2.5$) shown for the four vibrational frequencies $\omega_0 = 20, 30, 60$, and 90 .

4 the dynamic coefficient on the flexible bond for the four vibrational frequencies studied is compared with that on the rigid bond determined using Eq. (3.17). Clearly for sufficiently large ω_0 it is difficult to discern a difference between the two because whatever differences there are occur in the long time tail. For reference, we plot $\zeta_{sp}(t)/2$ in Fig. 5, where $\zeta_{sp}(t)$ is the friction experienced by a single Lennard-Jones particle in the fluid. Although the differences may appear small, they can give rise to large differences in the static friction values. The differences can be seen more clearly by plotting the real and imaginary parts of the Fourier-Laplace transform of the dynamic friction

$$\zeta(\omega) = \int_0^\infty dt \zeta(t) e^{-i\omega t} = \zeta'(\omega) - i\zeta''(\omega), \quad (4.8)$$

where $\zeta'(\omega)$ and $\zeta''(\omega)$ are respectively the real and imaginary parts. These are plotted in Fig. 6. The differences are most pronounced in the small frequency behavior of $\zeta'(\omega)$,

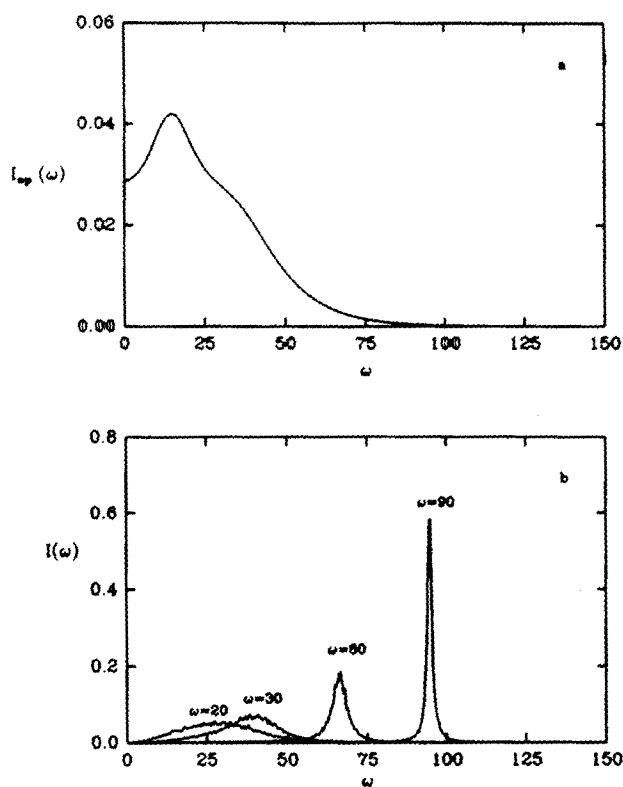


FIG. 2. (a) The spectral density of the velocity of a single solvent atom of Lennard-Jonesium at same density and temperature as in Fig. 1 computed from the analytic fit to the single-particle velocity autocorrelation function of Straub *et al.* (Ref. 15) using Eq. (4.7). (b) The spectral densities corresponding to the velocity autocorrelation functions in Fig. 1 computed using Eq. (4.7).

in particular, the values of $\zeta'(\omega = 0)$, which is, by definition, the static friction coefficient.

The analysis of Secs. II and III applies to the case in which the diatomic molecule is not allowed to rotate; rotations should not alter the results. To see this, we compare the dynamic friction on the rotational flexible and rigid diatom-

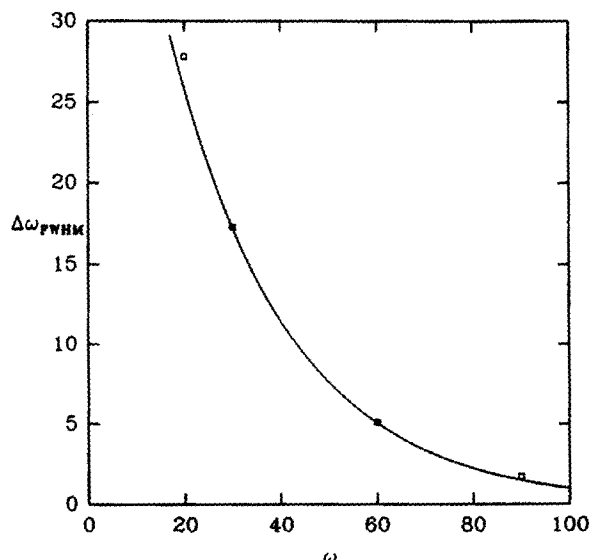


FIG. 3. A plot of the full width at half maximum, ω_{FWHM} vs frequency for the four spectra of Fig. 2(b). The curve is derived from a cubic spline fit to the data points.

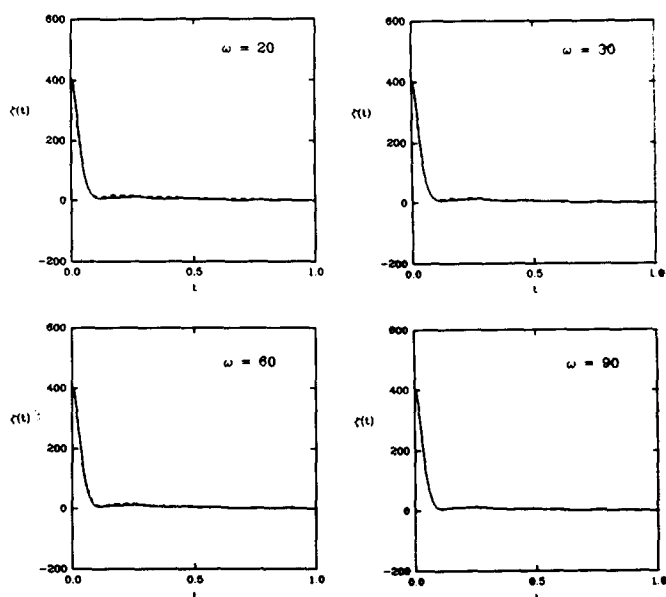


FIG. 4. Comparisons of the dynamic friction kernels for the nonrotational rigid and flexible diatomics at four different frequencies. The solid curve is the friction on the rigid diatomic computed from molecular dynamics simulations using Eq. (3.17). The dashed curves show the friction on the flexible diatomic for the four frequencies as indicated in the figure.

ics for frequencies $\omega_0 = 30, 60$, and 90 in Fig. 7. We see excellent agreement between the flexible and rigid cases at all three frequencies. It is of further interest to determine whether or not rotations will affect the friction of the bond. Figure 8 compares the dynamic friction for rotational and nonrotational dynamics for both flexible and rigid bonds. From the figure, we see that there are subtle differences that arise from rotations. Again, these differences will have a dramatic effect on the static friction coefficients.

V. DISCUSSION OF RESULTS

The analysis in Secs. II and III is for a nonrotational flexible diatomic molecule dissolved in a liquid in which the

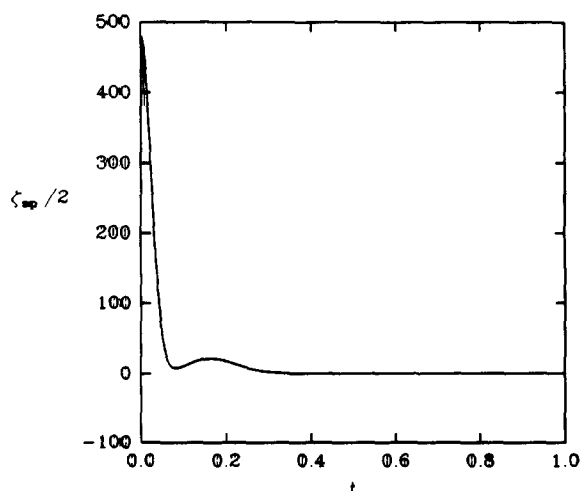


FIG. 5. The analytic fit to the dynamic friction kernel $\zeta_{sp}(t)/2$ for a single atom of Lennard-Jonesium ($\hbar = 1.05$, $\hat{T} = 2.5$) due to Straub *et al.* (Ref. 15).

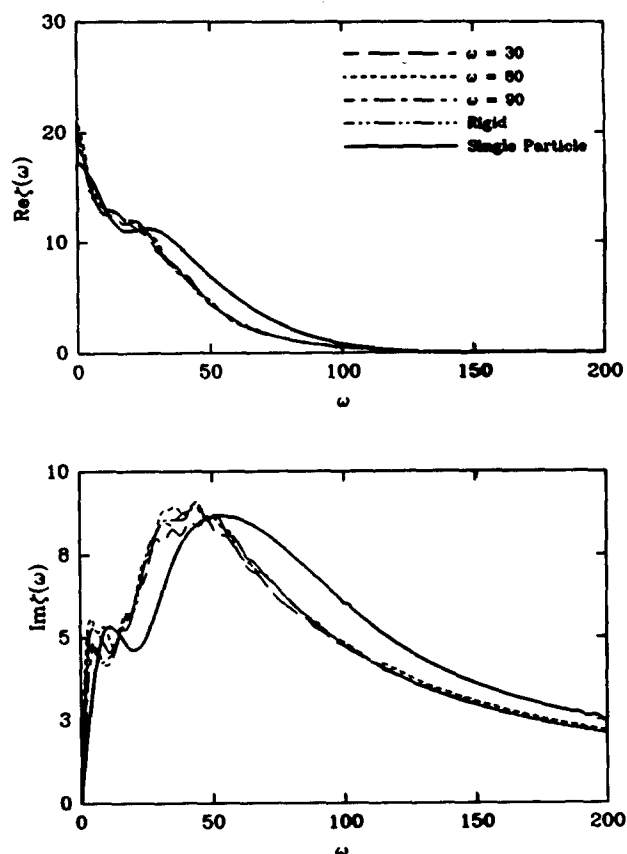


FIG. 6. Real and imaginary parts of the Fourier-Laplace transform $\zeta(\omega)$ of the dynamic friction kernels in Fig. 4 for the frequencies $\omega_0 = 30, 60$, and 90 , computed using Eq. (4.8). Also shown is the real and imaginary parts of $\zeta(\omega)$ for the rigid diatomic. The heavy solid lines are the real and imaginary parts of $\zeta_{sp}(\omega)/2$ for the single solvent atom, based on the analytic fit of Straub *et al.* (Ref. 15).

bond-potential can be anharmonic but must have a stable minimum. The resulting GLE [cf. Eq. (2.10)] correctly describes the anharmonic oscillator only when it is very close to equilibrium. In this eventuality the force is effectively harmonic, albeit with a renormalized harmonic frequency, $\tilde{\omega}$ [cf. Eq. (2.9)], which is given by the curvature of the potential of mean force at the potential minimum. When the molecule has a purely harmonic bond the potential of mean force will be

$$W(x) = \frac{1}{2} \mu \omega_0^2 (x - x_0)^2 - kT \ln y(x), \quad (5.1)$$

where $y(x)$ is the cavity distribution function. If the molecule is very stiff, that is, if $y(x)$ varies slowly compared to the bare quadratic potential, the GLE should be an excellent approximation to the dynamics of the system for initial states further from equilibrium than would be valid for a dissolved anharmonic oscillator. In this paper we treat only the case of a pure harmonic oscillator dissolved in Lennard-Jonesium. In a subsequent paper we shall treat anharmonic molecules where even a small anharmonicity has a dramatic effect on the dephasing decay.

The dynamic friction appearing in the GLE is given by Eq. (2.7) which involves a projected Liouville propagator. The fluctuating force, δf , consists of two parts: a part arising from the force on the bond, and a part representing the devi-

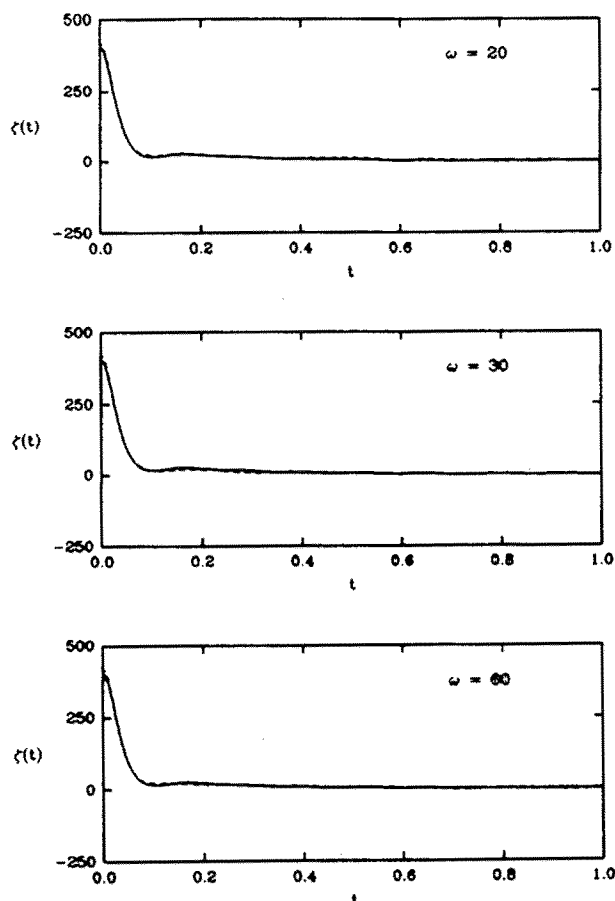


FIG. 7. Comparisons of the dynamic friction kernels for the rotational rigid and flexible diatomics at frequencies $\omega = 20, 30$, and 60 . The solid curve is the friction on the rigid diatomic computed from molecular dynamics simulations using Eq. (3.17). The dashed curves show the friction on the flexible diatomic for the three frequencies as indicated in the figure.

ation of the bare intramolecular force from the renormalized harmonic force on the bond. Equation (2.17) shows how $\zeta(t)$ is related to the autocorrelation function of the fluctuating force propagated with the true Liouville propagator. This relationship is useful for two reasons. First, from it one can derive an expression for the static friction on the bond in terms of the ordinary dynamics of the system, a result given by Eq. (2.21). This quantity is easy to calculate from MD trajectories. Second, it is a useful starting point for the ensuing asymptotic analysis based on the classical Born–Oppenheimer approximation which shows that in the limit $\omega_0 \rightarrow \infty$, $\zeta(t)$ is given by Eq. (3.1). In this limit one can compute the bond friction as follows: (1) Freeze the bond at the bare bond length x_0 ; (2) calculate the autocorrelation function of $\delta f^{(0)}(t) = (f^{(0)}(t) - \bar{f}^{(0)})$, where $f^{(0)}$ is the solvent force on the rigid bond. This is best done using MD with SHAKE or another equivalent constrained MD algorithm.

This is a very simple algorithm for approximating the bond friction. We must determine when this asymptotic result becomes valid. Figure 4 shows that for all the oscillator frequencies ($\omega_0 = 20, 30, 60$, and 90) studied the rigid bond approximation is excellent. This is very surprising since the lower frequencies, $\omega_0 = 20$ and 30 , fall near the peak of the spectral density of the neat solvent [see Fig. 2(a)]. For these frequencies the solute vibrations are not fast compared to the

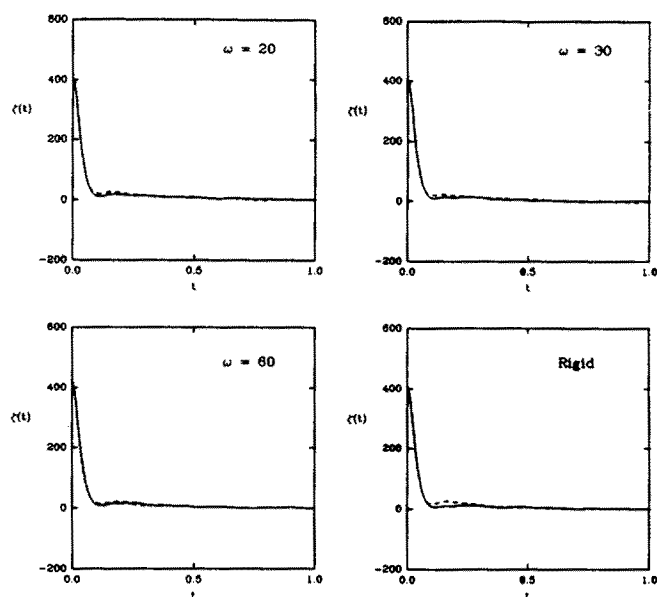


FIG. 8. Comparisons of the dynamic friction kernels for rotational and non-rotational diatomic molecules in Lennard-Jonesium. The first three plots show the comparisons for the flexible diatomic at the frequencies indicated. The last shows the comparison for the rigid diatomic.

solvent dynamics and the adiabatic analysis should not be valid. Why then is the asymptotic limit a good approximation to the true friction coefficient? In the discussion following the derivation in Sec. III we show that for an anharmonic oscillator coupled bilinearly to a harmonic bath, the dynamic friction on the oscillator is rigorously given by Eq. (3.20) and is thus independent of the oscillator frequency and of the temperature. Whether or not an effective harmonic bath model can describe dynamics in a real liquid can be tested by studying the dynamic friction on the vibrating bond as a function of temperature at constant liquid density. If there is no frequency or temperature dependence, it can be concluded that the effective harmonic bath model is a good description. We have already seen that $\zeta(t)$ is independent of the bond frequency, however, it turns out to be strongly temperature dependent. This was determined by performing simulations at four different temperatures for a bond frequency of 30 and density of 1.05 . For simulations done at temperatures $T = 1.74$ (just above the melting point for this density), 2.0 , 2.5 , and 3.0 , we find that $\zeta(t=0) = 286.03, 362.52, 402.74, 443.66$, and $\hat{\zeta}(\omega=0) = 15.97, 21.20, 20.13$, and 19.09 , respectively. We thus conclude that the effective harmonic bath Hamiltonian is not valid for the fluids studied here—more about this in a subsequent publication.

The foregoing analysis is based on the case of a diatomic molecule constrained not to rotate. Figure 7 shows that the rigid bond friction is still an excellent approximation even when simulations are done on molecules that are free to rotate. Interestingly, the friction on molecules allowed to rotate differs systematically from the friction on molecules not allowed to rotate. This is shown in Fig. 8 where we compare the friction coefficient on flexible molecules that can and cannot rotate. The last plate in the figure compares the friction on rigid rotational and rigid nonrotational bonds. In all

of these cases the deviation is largest at intermediate times. It is easy to see why rotations enter in the rigid bond case. The force on the rigid bond is then

$$f^{(0)}(t) = \frac{1}{2} \sum_{\alpha=1}^N \left[\mathbf{F}_{\alpha,1} \left(\left| \mathbf{r}_{\alpha} - \mathbf{R} + \frac{1}{2} x_0 \hat{\mathbf{u}} \right| \right) - \mathbf{F}_{\alpha,2} \left(\left| \mathbf{r}_{\alpha} - \mathbf{R} - \frac{1}{2} x_0 \hat{\mathbf{u}} \right| \right) \right] \cdot \hat{\mathbf{u}}, \quad (5.2)$$

where $\mathbf{F}_{\alpha,1}$ and $\mathbf{F}_{\alpha,2}$ are the forces exerted by fluid atom α on atoms 1 and 2 respectively of the diatomic molecule whose center of mass position is \mathbf{R} , bond length is fixed rigidly at x_0 , and orientation is defined by the unit vector, $\hat{\mathbf{u}}$, lying along the molecular axis. Clearly if the molecule can reorient $\hat{\mathbf{u}}$ changes direction and even if the solvent is frozen in place this force will fluctuate. For the case of the nonrotational molecule there will be no such contribution. This rotational component can make a small difference in the static friction coefficient. For example for the case presented here the static bond friction for the rigid rotational molecule is 21.4 and for the rigid nonrotational molecule is 19.7. It is of interest to investigate the spectral densities of the vibrational velocity. The velocity autocorrelation functions are given in Fig. 1 and the corresponding spectral densities are given in Fig. 2(b). From the GLE it is a simple matter to show that

$$I(\omega) = \frac{\omega^2 \gamma'(\omega)}{[\omega^2 - \tilde{\omega}^2 + \omega \gamma''(\omega)]^2 + [\omega \gamma'(\omega)]^2}, \quad (5.3)$$

where $\gamma(t) = \zeta(t)/\mu$, and $\gamma'(\omega)$ and $\gamma''(\omega)$ are the real and imaginary parts of the Fourier-Laplace transform of $\gamma(t)$ [cf. Eq. (4.8)].

Using the friction coefficient determined in the rigid bond approximation we can compute the spectrum predicted using Eq. (5.3). This is compared with the simulated spectrum in Fig. 9. Clearly, the GLE does very well. Shown also in this figure are the spectra predicted if the single particle friction is used—more about this later. These spectra were calculated using values of $\tilde{\omega}$ obtained from the MD

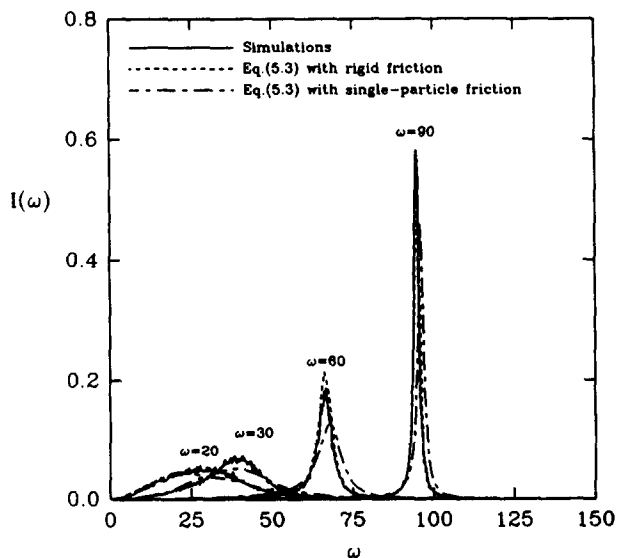


FIG. 9. Comparison of the measured spectrum in Fig. 2 to the spectrum predicted by the GLE in Eq. (5.3). The predicted spectra were computed using both the rigid friction and the single-particle friction in Eq. (5.3).

simulations using Eq. (2.9). The values are $\tilde{\omega} = 16.02, 27.73, 58.55$, and 89.48 for $\omega_0 = 20, 30, 60$, and 90 , respectively. Moreover the full width at half maximum predicted by the GLE is in excellent agreement with the simulation data.

In the Introduction we discussed the kind of stochastic modeling that is becoming increasingly popular. If each atom i in the diatomic molecule is assumed to obey a GLE of its own

$$m_i \ddot{x}_i = - \frac{\partial W}{\partial x_i} - \sum_{j=1}^2 \int_0^t d\tau \zeta_{ij}(t-\tau) \dot{x}_j(\tau) + R_i(t), \quad (5.4)$$

where $W(x)$ is the potential of mean force and $\zeta_{ij}(t)$ is the friction matrix. If the cross frictions are ignored ($\zeta_{12}(t) = \zeta_{21}(t) = 0$) and one transforms to center of mass and relative coordinates one obtains for a homonuclear diatomic molecule,

$$\mu \ddot{x} = - \frac{\partial W}{\partial x} - \int_0^t d\tau \frac{\zeta_{sp}(t-\tau)}{2} \dot{x}(\tau) + R(t), \quad (5.5)$$

where $\zeta_{sp}(t)$ is the friction on a single atom of the homonuclear diatomic molecule. This is obtained by dissolving this single atom in the solvent, determining its velocity autocorrelation function, and using the method of Berne and Harp²⁵ to determine the single particle friction. This is the free draining model of bond friction, a model that ignores cross correlations between the solvent forces on each atom of the diatomic. In this model the bond friction is given by,

$$\zeta(t) = \zeta_{sp}(t)/2. \quad (5.6)$$

We have already discussed when this might be a valid approximation. In Fig. 6, we present simulated $\zeta(\omega)$ and compare it with $\zeta_{sp}(\omega)/2$. Clearly for bond length $x_0 = 1.25$ studied here there are significant discrepancies in the free draining limit at all but high frequencies. These discrepancies show up in both the real and imaginary parts of $\zeta(\omega)$. To understand why there is agreement at high frequencies it is useful to look at the time dependence of $\zeta(t)$ in the figures. The short time decay is due to the very strong repulsive collisions between solvent atoms and the atoms of the diatomic. The time scale of this short time decay is the duration of a collision. These very strong repulsive collisions require the solvent atoms to be close to the molecular atoms. Collisions along the molecular axis will contribute to the friction much more strongly than collisions transverse to the molecular axis. Such collisions will take place when a solvent atom approaches from one end or the other. In such a collision the solvent atom will not simultaneously interact strongly with both molecular atoms, and these contributions should not be effected by cross-correlations and should thus be well approximated by the free draining model. Because these short time effects contribute only to the high frequency friction, we find that $\zeta'_{sp}(\omega)/2$ agrees well with the true $\zeta'(\omega)$ at high frequencies. Any phenomena dominated by these close-in collisions should be accurately described by an independent binary collision approximation. The long time behavior is due to collective hydrodynamic effects and should be poorly described by the free-draining model. In frequency space these hydrodynamic effects contribute to the low frequency

friction and there we see large deviations from the single particle free draining model. A sensitive test of the free draining model is shown in Fig. 9 where a plot of the spectra calculated by substituting $\gamma_{sp}(\omega) \equiv \zeta_{sp}(\omega)/2\mu$ into Eq. (5.3) is compared to the true spectra. It is clear from this comparison that the free-draining model fails.

ACKNOWLEDGMENTS

We have benefitted from very useful discussions with Profs. Philip Pechukas, Eli Pollak, Hermann Grabert, and Peter Hanggi and Glenn Martyna for his ideas on rotational NAPA discussed in the Appendix. This work was supported by a grant from the NSF (NSF CHE-87-00522 and by a grant from the American Chemical Society–Petroleum Research Foundation No. 19890.

APPENDIX

In this appendix, we show how the NAPA integration method can be applied to the case of a rotating molecule.

If \mathbf{r}_1 and \mathbf{r}_2 denote the positions of the two nuclei of the diatomic and the intramolecular potential is $\mathbf{r} = \mathbf{r}_1 - \mathbf{r}_2$ of the form

$$V(r) = \frac{1}{2} k(r - r_0)^2 \quad (\text{A1})$$

the Taylor series expansion to second order of the potential, $V(r)$, in Cartesian coordinates around the point (x_0, y_0, z_0) gives

$$V(x, y, z) = \frac{1}{2} \sum_{ij} K_{ij} (x_i - x_{i0}) (x_j - x_{j0}), \quad (\text{A2})$$

where the force constant matrix is

$$K_{ij} = k x_{i0} x_{j0} / r_0^2. \quad (\text{A3})$$

If the oscillator is very stiff, then this second order expansion is a reasonable approximation to the original potential $V(r)$. From the definition of K_{ij} , the following properties can be easily verified:

$$\begin{aligned} K_{ij} &= K_{ji} \\ K_{ii} K_{jj} &= K_{ij}^2 \end{aligned} \quad (\text{A4})$$

$$\sum_i K_{ii} = k.$$

Transformation to normal modes diagonalizes the 3×3 matrix K_{ij} . The normal mode frequencies are

$$\begin{aligned} \omega_1^2 &= \omega_2^2 = 0 \\ \omega_3^2 &= K_{xx} + K_{yy} + K_{zz} = k, \end{aligned} \quad (\text{A5})$$

where the two zero frequency modes correspond to the two rotational degrees of freedom while ω_3 corresponds to the single vibrational degree of freedom. Because of the degeneracy in the eigenvalues, a Gram-Schmidt orthogonalization procedure may be used to obtain the corresponding eigenvectors from which the unitary transformation \mathbf{U} to normal coordinates can be constructed in the usual way. If \mathbf{x} denotes the vector of Cartesian components and \mathbf{q} denotes the vector of normal mode coordinates, then the transformation is written

$$\mathbf{x} = \mathbf{U}\mathbf{q}. \quad (\text{A6})$$

When written in terms of the q_s , the potential becomes a function of q_3 alone

$$V(q_3) = \frac{1}{2} k q_3^2. \quad (\text{A7})$$

The NAPA method¹⁶ is used to integrate the q_3 equation, while the q_1 and q_2 equations can be integrated by any of the standard methods (for example the velocity Verlet integrator). Then the unitary transformation \mathbf{U} is used to transform back to Cartesian coordinates in terms of which the forces due to the solvent are computed.

Since the only parameters in the harmonic potential Eq. (A1) are the force constant k and the minimum r_0 , the choice of the Cartesian components x_{i0} is arbitrary so long as they satisfy

$$x_0^2 + y_0^2 + z_0^2 = r_0^2. \quad (\text{A8})$$

It is found that the best choice for use with the NAPA integrator is

$$x_{i0} = \frac{x_i}{r} r_0. \quad (\text{A9})$$

Substituting this choice into Eq. (A3), the matrix elements K_{ij} become

$$K_{ij} = k x_i x_j / r^2. \quad (\text{A10})$$

We see that the matrix elements K_{ij} are no longer constants, but depend explicitly on the coordinates associated with the diatomic at a given time step. Although the normal mode frequencies remain independent of the coordinates, the transformation matrix \mathbf{U} must be recomputed at every time step. However, since this calculation is relatively simple, the extra time spent will not be a significant disadvantage.

¹ B. J. Berne and R. Pecora, *Dynamic Light Scattering* (Wiley-Interscience, New York, 1976).

² P. Hänggi, P. Talkner, and M. Borkovec, *Rev. Mod. Phys.* **62**, 250 (1990).

³ J. T. Hynes, in *Theory of Chemical Reaction Dynamics*, edited by M. Baer (CRC Press, Boca Raton, FL, 1985), p. 171.

⁴ R. Zwanzig and M. Bixon, *Phys. Rev. A* **2**, 2005 (1970).

⁵ B. J. Berne, *J. Chem. Phys.* **56**, 2164 (1972).

⁶ H. Yamakawa, *Modern Theory of Polymer Solutions* (Harper and Row, New York, 1971).

⁷ R. I. Cukier, R. Kapral, and J. R. Mehafeff, *J. Chem. Phys.* **73**, 5254 (1980).

⁸ M. Schell, R. Kapral, and R. I. Cukier, *J. Chem. Phys.* **75**, 5879 (1981).

⁹ D. E. Smith and C. B. Harris, *J. Chem. Phys.* **92**, 1304 (1990).

¹⁰ D. E. Smith and C. B. Harris, *J. Chem. Phys.* **92**, 1312 (1990).

¹¹ J. A. Montgomery, Jr., D. Chandler, and B. J. Berne, *J. Chem. Phys.* **70**, 4056 (1979).

¹² J. A. Montgomery, Jr., S. L. Holmgren, and D. Chandler, *J. Chem. Phys.* **73**, 3866 (1980).

¹³ J. E. Straub, M. Borkovec, and B. J. Berne, *J. Phys. Chem.* **91**, 4995 (1987).

¹⁴ J. Straub, B. J. Berne, and Benoit Roux, *J. Chem. Phys.* (1990).

¹⁵ J. E. Straub, M. Borkovec, and B. J. Berne, *J. Chem. Phys.* **89**, 4833 (1988).

¹⁶ M. Tuckerman, G. Martyna, and B. J. Berne, *J. Chem. Phys.* **93**, 1287 (1990).

¹⁷ J. P. Bergsma, B. J. Gertner, K. R. Wilson, and J. T. Hynes, *J. Chem. Phys.* **86**, 1356 (1987).

¹⁸ H. Mori, *Prog. Theor. Phys.* **33**, 423 (1965).

¹⁹ B. J. Berne, in *Physical Chemistry, An Advanced Treatise XI B*, edited by H. Eyring, D. Henderson, and W. Jost (Academic, New York, 1971).

²⁰ J. T. Hynes and J. M. Deutch, *Physical Chemistry, An Advanced Treatise XI B*, edited by H. Eyring, D. Henderson, and W. Jost (Academic, New York, 1975).

²¹ H. Grabert, in *Projection Operator Techniques in Nonequilibrium Sys-*

- tems, Springer Tracts in Modern Physics, Vol. 95*, edited by G. Höhler (Springer, Berlin, 1982).
- ²² P. Pechukas, *J. Chem. Phys.* **72**, 6320 (1980).
- ²³ R. Zwanzig, *J. Stat. Phys.* **9**, 215 (1973).
- ²⁴ J. M. Deutch and R. Silbey, *Phys. Rev. A* **3**, 2049 (1971).
- ²⁵ B. J. Berne and G. D. Harp, *Adv. Chem. Phys.* **17**, 63 (1970).
- ²⁶ L. Verlet, *Phys. Rev.* **159**, 98 (1967).
- ²⁷ H. C. Andersen, *J. Compt. Phys.* **52**, 24 (1983).
- ²⁸ G. Ciccotti, J. P. Ryckaert, and H. J. C. Berendsen, *J. Compt. Phys.* **23**, 327 (1977).
- ²⁹ W. F. van Gunsteren and H. J. C. Berendsen, *Mol. Phys.* **34**, 1311 (1977).
- ³⁰ W. C. Swope, H. C. Andersen, P. H. Berens, and K. R. Wilson, *J. Chem. Phys.* **76**, 637 (1982).
- ³¹ R. P. Futrelle and D. J. McGinty, *Chem. Phys. Lett.* **12**, 285 (1971).